





Spatial Investigation of Soil Erosion Risk in the High Rainfall Zone of Pakistan by Using Rusle Model

Ihtisham Khan^{1*}, Muhammad Fahad Bilal², Shahid Ghazi², Kashif Khan¹, Muzamil Khan³,

- ¹ School of Geosciences and Info Physics, Central South University, Changsha, 410083, China
- ² Centre for Geographical Information System, University of the Punjab, Lahore, 54000, Pakistan
- ³ Department of Geology, Bacha Khan University Charsada, 24420, Pakistan
- *Corresponding Author: geologistihtisham@gmail.com

Citation | Khan. I, Bilal. M. F, Ghazi. S, Khan. K, Khan. M, "Spatial Investigation of Soil Erosion Risk in the High Rainfall Zone of Pakistan by Using Rusle Model", IJIST, Vol. 6 Issue. 2 pp. 532-549, May 2024

DOI https://doi.org/10.33411/ijist/202462532549

Received | April 25, 2024 Revised | May 09, 2024 Accepted | May 16, 2024 Published | May 28, 2024.

The degradation of soil quality and agricultural sustainability is threatened by soil erosion, which poses a serious threat to livelihoods and food security. Maintaining soil fertility and reducing the danger of erosion require efficient evaluation and management strategies. This research presents an innovative approach to assess soil erosion in Nowshera District, leveraging remote sensing technology coupled with Geographic Information System (GIS) tools. The study intends to offer a thorough and accurate understanding of erosion patterns and drivers in the area by incorporating these cutting-edge approaches. Cloud-free LANDSAT 8 multispectral images, characterized by minimal vegetation cover, serve as the primary dataset for this analysis. The integration of the RUSLE model with GIS and remote sensing techniques enables the calculation of soil erosion rates throughout the research region. The study demonstrates variation in soil erosion parameters across different locations, as indicated by R factor values, which range from 603.43 to 696.43 MJ mm/ha/h/year. The southeastern portion demonstrates significantly lower erosion rates than the northwestern part, which can be linked to variations in topography and land use patterns. This study highlights the significance of using remote sensing techniques to evaluate soil erosion changes over time and provide valuable information for land management plans in Nowshera District, Pakistan. The study results can prove valuable during decision-making regarding conservation planning and agricultural sustainability.

Keywords: Geospatial Analysis, Remote Sensing, Revised Universal Soil Loss Equation (RUSLE), Soil Erosion, Landsat.











INFOBASE INDEX



















Introduction:

Soil erosion, a widespread phenomenon with spatial and temporal consequences, is closely connected to the deterioration of land resources [1]. It is the most prevalent land degradation concern, affecting soil quality and crop output [2]. Approximately 1100 million hectares of land worldwide are impacted by affected by water-induced soil erosion, of which 56% is affected due to degradation of soil caused by human activities. Soil degradation threatens 441 million hectares of land (59%) in Asia [3]. Agricultural productivity is negatively impacted in many countries due to the loss of topsoil from erosion. Soil erosion can be caused by natural geomorphic processes and anthropogenic actions [4]. Water-induced soil erosion occurs through various mechanisms such as gullies, rills, mixing processes, landslides, riverbank erosion, and sheet erosion. Nevertheless, the primary contributing factors include deforestation, improper land use, excessive grazing, poorly managed agricultural practices, and increased urbanization [5]. Changes in the climate, steep slopes, or basic soil properties increase the danger of soil erosion [6]. The interaction of slope significantly influences the runoff mechanism, with an increased slope leading to higher runoff and reduced infiltration, thus contributing to erosion.

The varieties of vegetation in an area can either contribute to erosion control or increase susceptibility to it. Certain plants, in particular, those with extensive root systems can aid in stabilizing the soil and halting erosion by holding it in place. However, in areas where erosion is prevalent, these plants may be eroded, which can lead to a decline in plant growth rates [7]. The characteristics of the soil, such as its texture and composition, play a critical role in water-induced soil erosion. Highly fertile soils are often targeted by flash floods and sheet erosion, which results in a significant loss of valuable nutrients from the soil. Additionally, soil with more permeable subsurface layers can result in increased amounts of water runoff, diminishing the availability of water for plant development. The way land is managed and utilized can either exacerbate or mitigate water-induced soil erosion. Unsustainable land use practices, such as deforestation or improper agricultural methods, can disrupt the natural balance and make soil more susceptible to erosion. Consequently, negatively impacting the plant growth rates and the overall health of the ecosystem [8].

Soil erosion is a major disaster in semiarid regions [9], and lies among the most important concerns in ecology, natural resources, and agricultural growth [10]. There are numerous sources of silt and a scarcity of water in these areas [11]. Due to reservoir siltation, the excessive sediment intake in upstream rivers shortens the lifespan of dams, degrades the quality of the water, and inhibits biological activity [12]. Many methods used in the past to quantify soil degradation at the watershed scale rely on labor-intensive, expensive physical surveys, soil erosion susceptibility mapping is one of these essential methods. These conventional techniques included erosion pins, sediment traps, and sediment sampling, among others. Although these techniques offered insightful information about soil erosion, they frequently had drawbacks in terms of precision, cost, and scalability, especially when evaluating water-induced soil degradation at the watershed scale. Planning for soil management and conservation, as well as determining the environmental effects, requires a quantitative estimation of soil erosion at the regional level [13]. The main challenge with erosion risk models is their validation, primarily due to insufficient data for comparing model estimations with actual soil losses [14]. The current study aims to evaluate the Revised Universal Soil Loss Equation (RUSLE), which is based on Geographic Information Systems (GIS) and is used to calculate the average yearly soil loss in Nowshera. When calculating soil loss in smaller regions, such as fields and hillslopes, RUSLE is a popular and appropriate technique [15].

Objectives:

The primary objective of this study is to evaluate the patterns of soil erosion in the Nowshera District, Pakistan. It suggests efficient conservation methods to reduce erosion hazards and improve agricultural sustainability. The study seeks to measure soil loss rates by



utilizing remote sensing techniques and the Revised Universal Soil Loss Equation (RUSLE) model. Additionally, it attempts to combine satellite imagery with Geographic Information System (GIS) tools to identify areas susceptible to erosion and zones at risk of erosion.

Novelty:

This study presents a novel approach for evaluating soil erosion in Nowshera District, Pakistan. The method combines advanced remote sensing techniques with the Revised Universal Soil Loss Equation (RUSLE) and Geographic Information System (GIS) tools. The novel aspect of this approach is the utilization of remote sensing technologies to gain a thorough understanding of erosion dynamics in the region. This method is more precise and efficient compared to conventional ground-based surveys. The study seeks to utilize satellite imagery and topography data to improve our comprehension of erosion processes, pinpoint regions at risk, and enable focused conservation initiatives for sustainable land management.

Material and Methods:

Study Area:

The research was carried out in the district Nowshera, situated within the Khyber Pakhtunkhwa province of Pakistan, focusing on the critical issues of soil erosion and land degradation. District Nowshera is located in the province's east, next to district Peshawar. The geographic coordinates are 30° 25' 12" to 34° 5' 24" N latitude and 71° 24' 36" to 72° 9' 0" E longitude. Geographically, the region exhibits a diverse topography. The northern side of the district is primarily made up of plains with a vast network of rivers and canals. On the other hand, the southern areas, including Ziarat Kaka Sahib, Nizampur, and Cherat, have moderate hills and slopes, mostly rely on rainfall for their water supply, and frequently face water shortages. Because of the variation in the topography, certain places are more likely to experience waterlogging, while others experience ongoing water shortages. This study explores the complex issues brought about by these regional and environmental changes in the district as shown in Figure 1. The distribution of meteorological stations is shown in Figure 2.

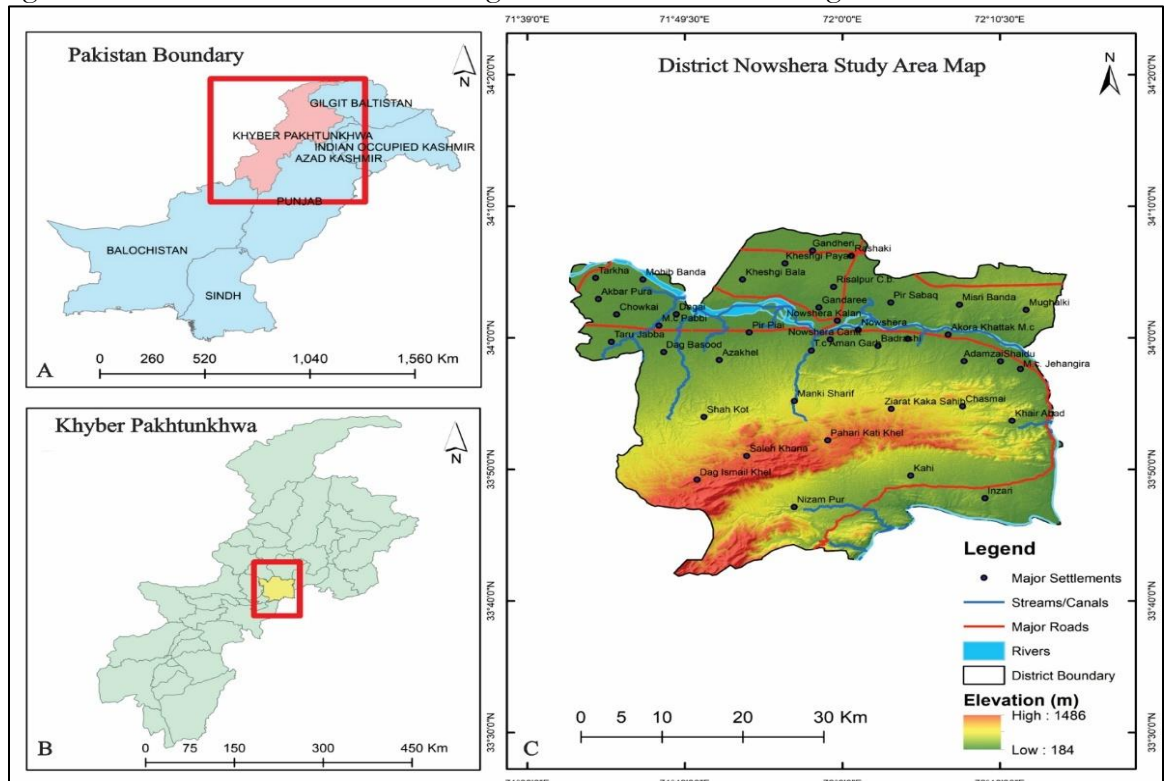


Figure 1: The study area location map (A) displays the Pakistan boundary line (B) denotes the study area province boundary (C) the study area district Nowshera



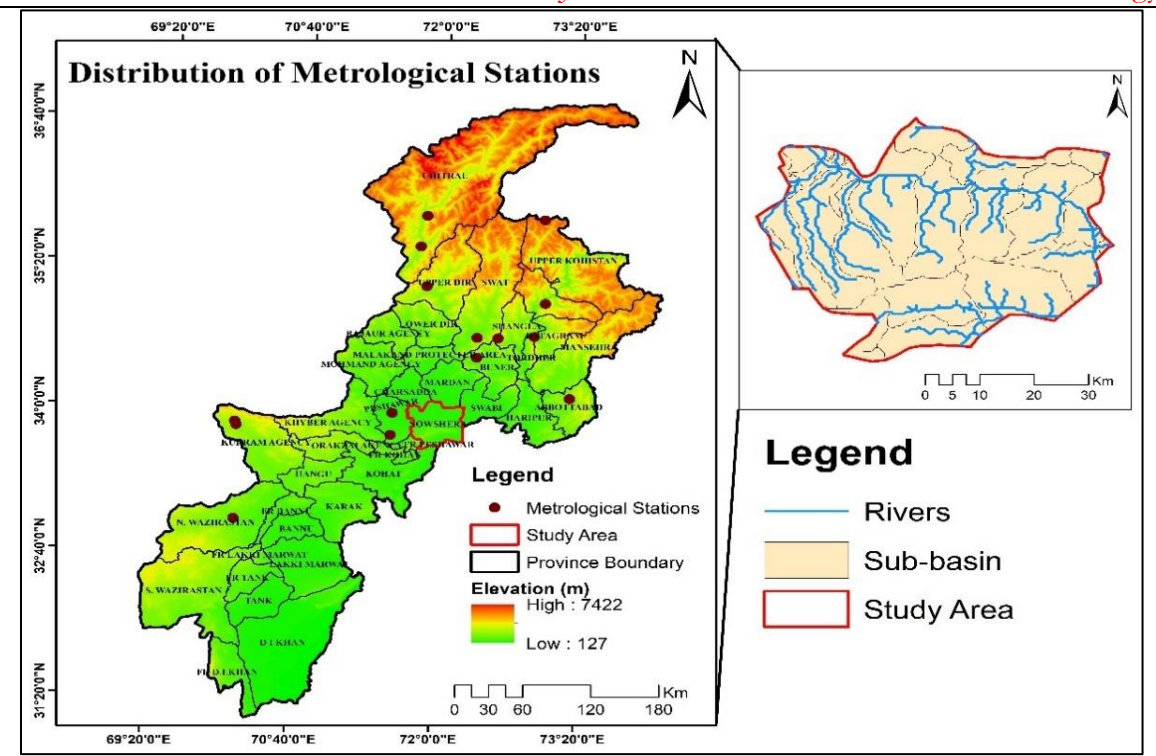


Figure 2: Distribution of the metrological stations across the study area

Data Acquisition and Processing:

A comprehensive dataset was compiled from various sources to facilitate a thorough analysis. Notably, topographic maps were acquired from the United States Geological Survey (USGS) through Earth Explorer, aligning with the methodological framework detailed in Figure 3. Field surveys were conducted in the Nowshera district to collect primary data, where careful observations and on-site data documentation were carried out. In addition, secondary data was gathered from other credible sources. The Pakistan Meteorological Department (PMD) provided meteorological data, which is essential for meteorological information. Soil-related data was provided by the Directorate of Soil Survey KP, which gave important insights into the properties of the soil. Information regarding the taxonomy and classification of soil was obtained from the Food and Agriculture Organization (FAO). Furthermore, satellite imagery, specifically Landsat 8 images from the USGS, was integrated to enhance the dataset.

Table 1: The data sets used in this study along with their sources

| Data Sets | Data Sources |
|------------------|--|
| Rainfall map | Pakistan Metrological Department (PMD) |
| Soil texture map | Directorate of Soil Survey Khyber Pakhtunkhwa, Pakistan. |
| | Food and Agriculture Organization (FAO); Digital soil |
| | map of the world database |
| DEM | Landsat-8 imagery (2020) 30m-spatial resolution. (USGS) |
| | https://earthexplorer.usgs.gov/ |
| LULC | Landsat-8 imagery (2020) 5m-spatial resolution (USGS) |

Data Analysis

The collected data underwent extensive processing and analysis. Quantitative techniques were applied using Microsoft Excel spreadsheets, wherein parameters related to the erosion model and land use were systematically encoded. Cartographic techniques were employed to ensure precision in the geospatial analysis of the collected data and to build data tables. High-precision data analysis and visualization were made possible by the implementation of these techniques, which were greatly aided by ArcGIS (10.8).



Flow of methodology diagram.

RUSLE Parameters:

The author [16] developed the following empirical soil loss model to forecast the average yearly soil loss over the long term in any given region.

$$A = R \times K \times LS \times C \times P \tag{1}$$

Whereas,

A = average annual soil loss (mg ha⁻¹ year⁻¹)

 \mathbf{R} = rainfall erosivity index (mm ha⁻¹ year⁻¹)

 $\mathbf{K} = \text{soil erodibility factor (mg ha}^{-1} \text{ year}^{-1})$

LS = topographic factor (dimensionless)

S stands for slope, and **L** for slope length.

C = Cropping factor (dimensionless)

P = Conservation practice factor (dimensionless)

Rainfall Erosivity (R):

The R factor explains how rainfall affects runoff and erosion. According to [17], it also describes the sizes and intensities of specific rainfall events for a year. The R index was calculated using the average annual rainfall (mm) of the Peshawar, Risalpur, and Cherat metrological stations from September 01, 2020, to September 30, 2020. In ArcGIS 10.8, the Inverse Distance Weightage (IDW) approach was used for spatial interpolation of rainfall data to represent the R factor spatially. The R factor was determined using Rainfall intensity and frequency since they are more predictive than the total amount of rainfall [18].

Table 2: The mean annual rainfall factor (R) of three metrological stations

| Rainfall Gauge Station | Latitude and Longitude | Elevation (m) | Annual Rainfall (mm) |
|---------------------------|----------------------------|---------------|----------------------|
| Peshawar | 71° 33′ 56″ E 34° 0′ 54″ N | 345 | 429.1 |
| Cherat | 72° 0′ 28" E 33° 50′ 21"N | 520 | 628.1 |
| Risalpur | 71° 59' 29" E 34° 03'42" N | 309 | 774.7 |

To estimate the R factor, 1-min rainfall data were first gathered. The product of the storm's maximum 30-min intensity (I30) and total kinetic energy (E) yields the amount of erosion that occurs during a single storm. According to [19], the R factor is defined as the total of the event EI30 values throughout a year. The 30-min rainfall erosivity index (EI30) was determined using the following formula, which was developed by Brown and Foster (1987):

$$EI_{30} = (\sum e_r \ v_r)I_{30}.$$
 (2)

$$e_r = 0.29[1 - 0.72 \exp(-0.05 i_r)]$$
 (3)

Where v_r (mm) is the amount of rainfall, i_r (mm h^{-1}) is the intensity, and I_{30} is the highest continuous 30-min rainfall intensity (mm h^{-1}) in a storm. EI_{30} is the 30-min rainfall erosivity index (MJ mm $ha^{-1}h^{-1}$), and er (MJ ha^{-1} mm⁻¹) is the unit energy (energy per unit of rainfall).

$$R = \frac{1}{n} \sum_{i=1}^{n} \sum_{j=1}^{n} (E I_{30}) ij.$$
 (4)

Where m was the number of erosive storms in the j_{ij} year and n was the length of the effective years.

Soil Erodibility (K):

According to [19], the K factor illustrates how susceptible certain soil types are to erosion and runoff rates. Since it indicates how soil particles are bound together, how cohesive or sticky they are, and how likely a certain soil is to erode on a particular slope, the K factor cannot be changed. Each type of soil has a different rate of erosion depending on its physical properties, including organic matter and texture [20]. Soil map from the Soil Survey of Pakistan served as the basis for the creation of a texture map of the district Nowshera. K values of 0.05 to 2.0 mm for sand, 0.002-0.05 mm for silt, and 0.002 mm for mud were used. K value for water bodies was considered as 0 because it has no estimated erosion value [21].



$$K = 0.1317 \times \frac{0.00021 \times M^{1.14} \times (12 - 0M) + 3.25(C_{\text{soilstr}} - 2) + 2.5(C_{\text{perm}} - 3)}{100}$$
 (5)

Where M is the textural factor calculated using equation (6)

$$M = (\%m_{silt} + \%m_{vfs}) * (100 - \%m_c)$$
 (6)

Where m_{silt} is the percentage fraction content of silts (0.002-0.5 mm), m_{vfs} is the percentage fraction content of fine sand (0.05-0.1 mm), m_c is the percentage fraction content of clay, and OM stands for soil organic matter (%). The USDA provides the soil structure code, $C_{soilstr}$, and the profile permeability class, C_{perm} .

Table 3: The K factor values of the soil of District Nowshera.

| SNUM | Texture | Clay1 | Silt1 | Sand1 | HYDGRP |
|------|------------|-------|-------|-------|--------|
| 3512 | Sandy Loam | 19 | 19 | 62 | С |
| 3843 | Clay Loam | 28 | 29 | 43 | С |
| 3871 | Clay | 48 | 29 | 23 | D |

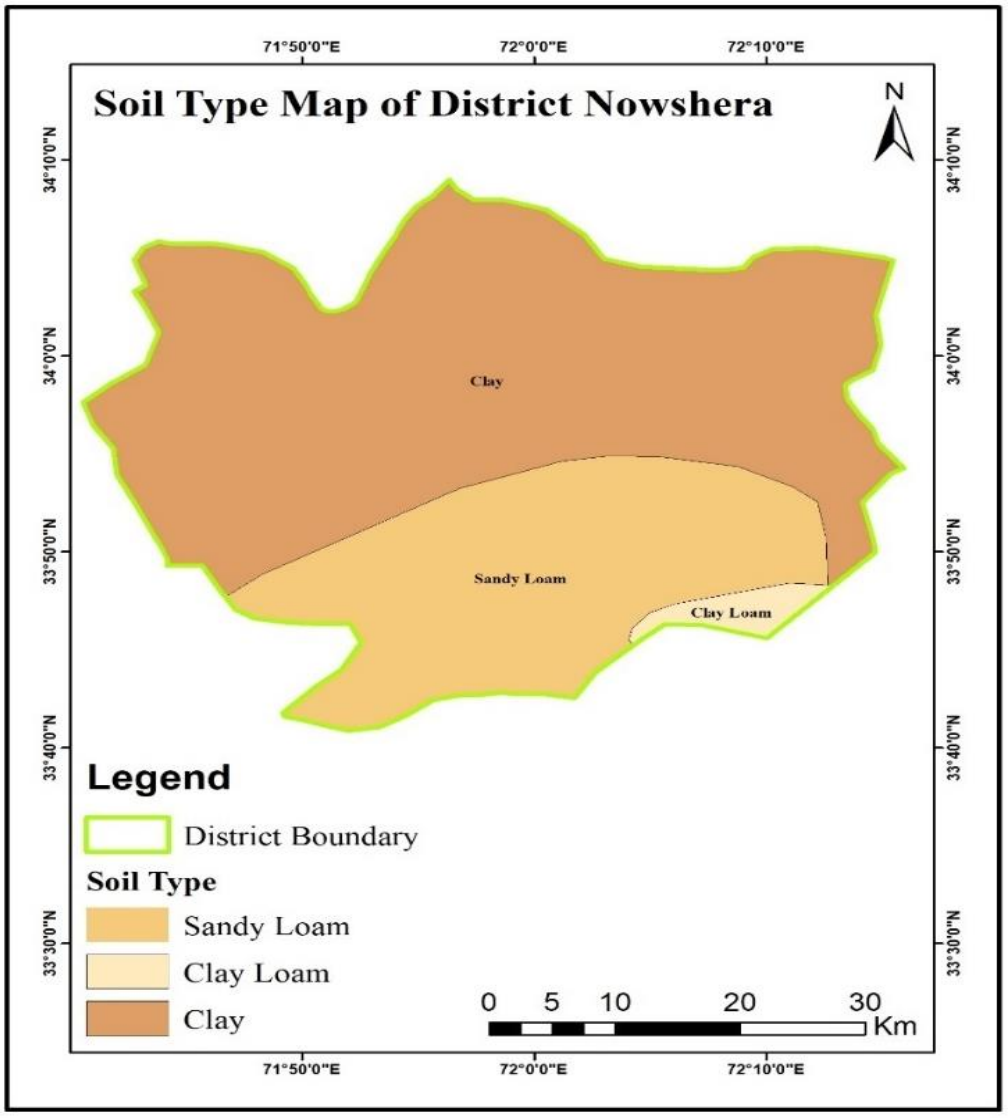


Figure 3: Soil type map of district Nowshera for calculating K factor.

Length of Slope (LS):

Ground-based models can be substituted with DEM processing in ArcGIS to determine the length and slope [22]. Slope steepness has a direct impact on erosion since a steeper slope erodes more quickly. DEM data was generated from Google Earth using points collected within the research area, and it was saved in KML format. Elevation data was then transferred to



https://www.gpsvisualizer.com/ and saved in gpx format. The gpx file was converted to a point feature in ArcGIS, and values were supplied to the closest vacant area between points using the Interpolation (kriging) tool. A five-meter-resolution raster elevation model was created. Errors such as sink and gaps in the DEM were eliminated by using the Arc hydro tool in ArcGIS to compute direction and flow accumulation.

$$LS = \left(FA \times \frac{\text{cellsize}}{22.13}\right)^{m} \left(\text{sin slope } \times \frac{0.01745}{0.0896}\right)^{n}, \quad (7)$$

LS is the slope length and steepness factor. FA is the flow accumulation utilized to calculate the upslope contributing component. Cell size is the resolution of the DEM in meters (for the present study, ≈ 5 m), slope is the slope raster in degree, m value range: 0.4–0.56; and n value range: 1.2–1.30. Flow of study diagram is shown in Figure 4.

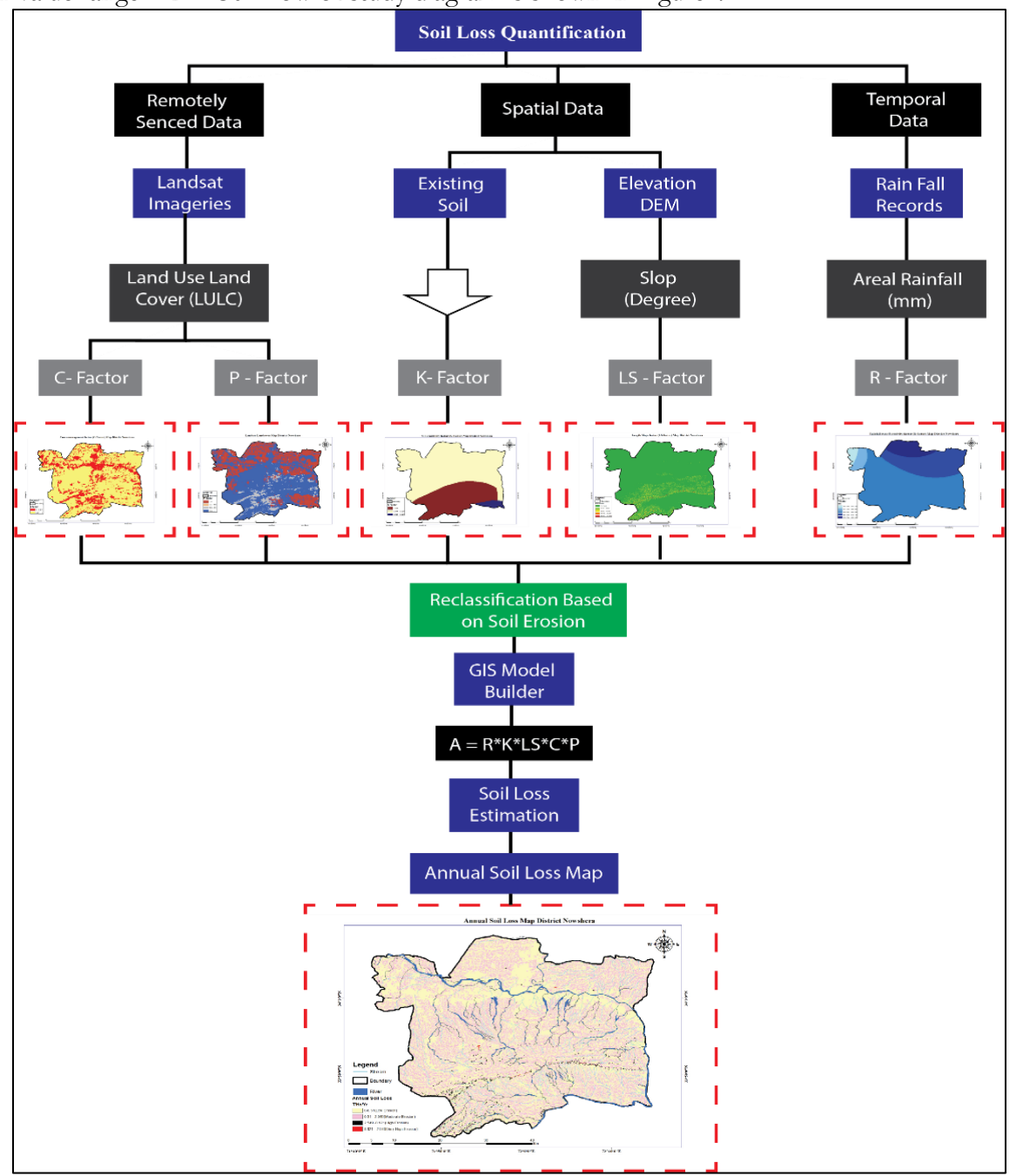


Figure 4: Methodological flow chart for evaluating annual soil loss using the RUSLE Model in district Nowshera, Pakistan



Cover Management/Crop Factor (C):

According to certain types of plants, crop management determines the soil losses [3] Landsat-8 image of the study area underwent supervised classification to identify Land Use And Land Cover (LULC). The LULC classes include forest, agriculture areas, barren land, populated areas, and water bodies. Average C-factor values for LULC types in the research region were computed by [23]. Field surveys were conducted to verify the Land Use Land Cover (LULC) classes and to provide ground truth data for accuracy evaluation. The C factor map was then generated by applying the following equation using the Raster Calculator tool [24].

$$C = \exp\left(-\alpha \times \frac{NDVI}{\beta - NDVI}\right),\tag{8}$$

Where NDVI is the Normalized Difference Vegetation Index and α and β are unit-less factors that determine the shape of the NDVI-C curve.

Support Factor (P):

The support factor (P) represents an association with a particular soil type. It illustrates the results of land use techniques that lessen runoff and, consequently, the rate of erosion. The P-factor displays the ratio of soil loss caused by a support method to that of straight-row farming both up and downhill [16]. The most popular supporting cropland practices are contour farming, cross-slope agriculture, terracing, and strip cropping [3]. The type of land used and the slope % are taken into consideration while choosing management practices to minimize soil loss. In this study, crops, shrubs, and wooded areas were categorized as agriculture zones, and P-factor values were calculated [16]. The P factor has a value between 0 and 1, where a value around 0 denotes good conservation practices and a value nearing 1 denotes poor conservation practices.

Results:

Rainfall Erosivity:

Rainfall erosivity measurements range from 603.4 to 696.43 MJ mm/ha/h/year. The northeast and surrounding areas have high precipitation intensities, according to the R factor map. Rainfall with high intensity can increase runoff, which in turn increases soil erosion in these regions as shown in Figure 5.

Soil Erodibility

In the research region, sandy loam predominates. The poor particle connectivity in silt loam contributes to its high erodibility, because of the built-up cover. However, due to their weak structure and low aggregation, salt-affected soils are extremely erodible. High K factor soils include cracked, patchy, and gully soils. The value of K ranges from 0.018 to 0.020 t·ha·h·ha⁻¹·Mj⁻¹·mm⁻¹ as shown in Figure 6.

Length of Slope:

The slope in the research area varies due to the shifting topography, resulting in intermittent slopes. Toward the southeast, there are steep slopes and high elevations. The research region displays both gradual and abrupt slopes due to its uneven topography. The range of values for the LS factor is 2.41 to 153.9, reflecting the complexity of the topography and the presence of steep slopes. This combination of complicated terrain and steep slopes heightens the region's vulnerability to soil loss, as depicted in Figure 7.



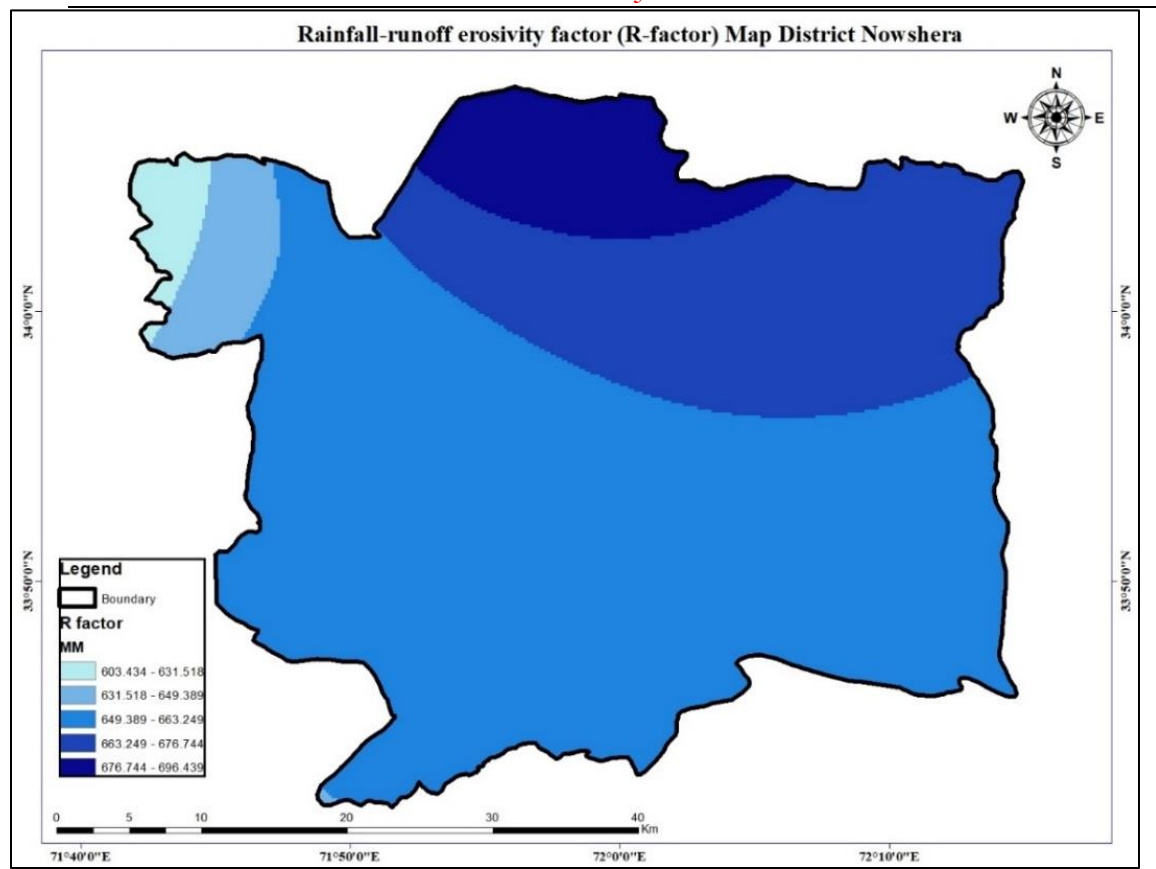


Figure 5: Rainfall factor (R) estimation in the study area

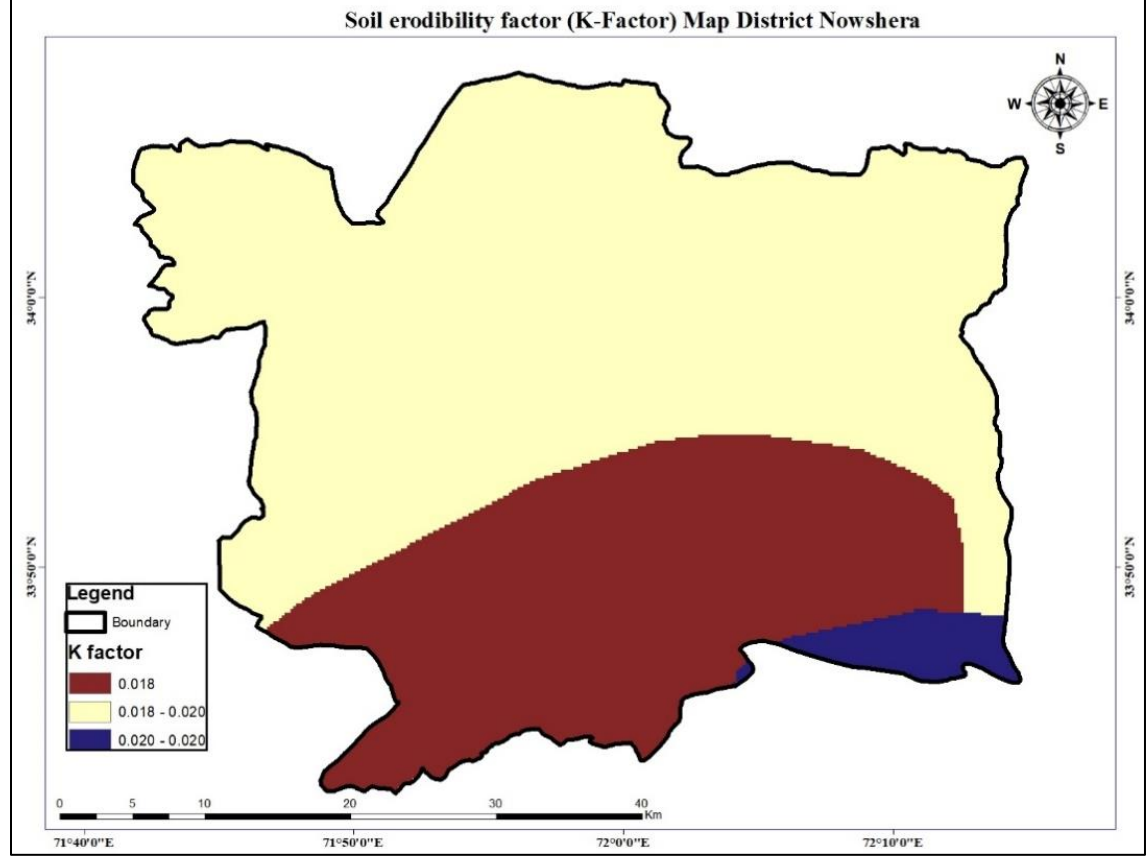


Figure 6: Erosion factor (K) estimation in the study area



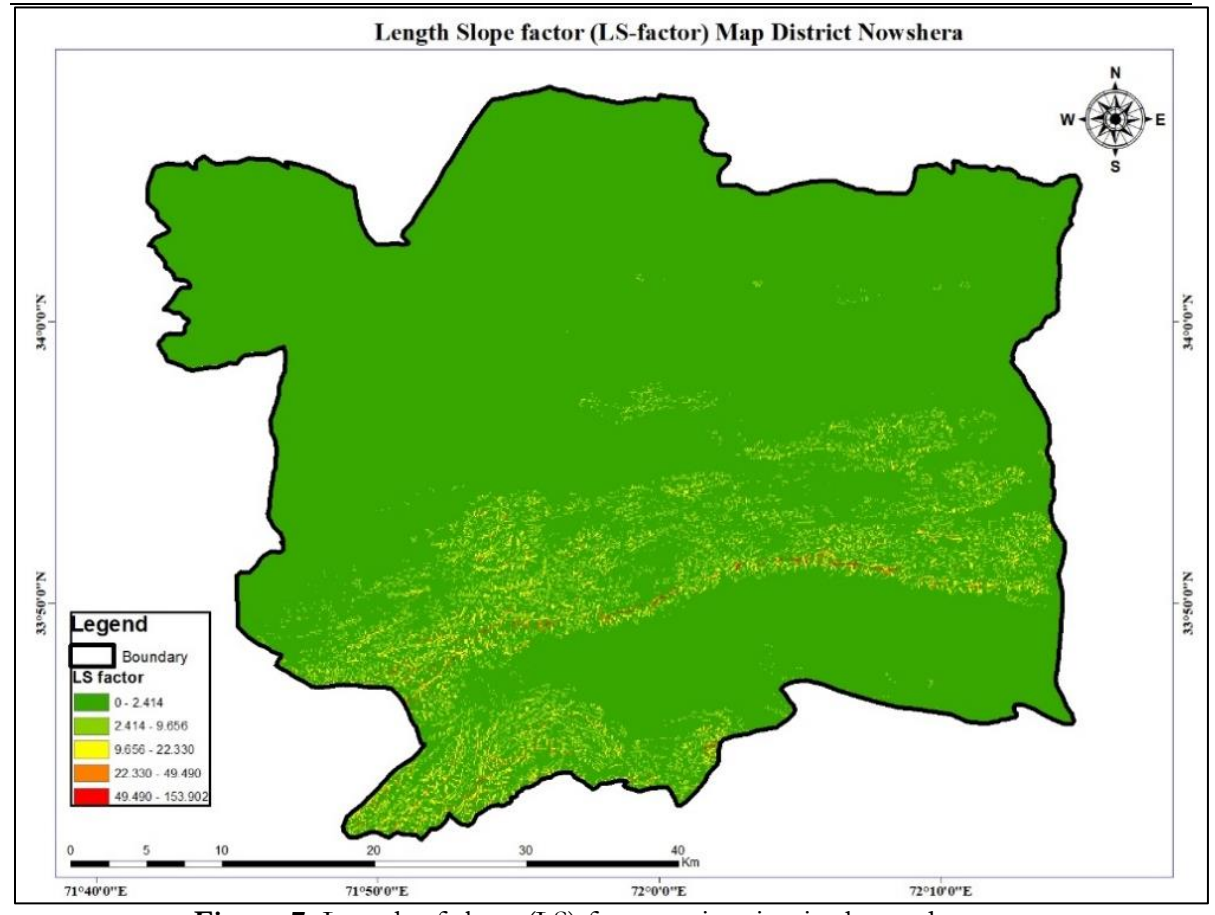


Figure 7: Length of slope (LS) factor estimation in the study area

Crop Factor:

Application of supervised classification to a 2020 Landsat image allowed for the identification of major land use types. Digital image processing was done using ArcGIS, complemented by field observations to validate the land use classes found on Google Earth. In the research region, the C factor values range from 0 to 1 as shown in figure 9. The western part of the study area exhibits high C factor on level surfaces, with significant values assigned to the forest, shrub, and thin forested region. The C factor values for land cover and land use are shown in Table 4 below. **Table 4:** The C factor values for land cover and land use in the study

| area | | | | |
|-------------------|----------|--|--|--|
| Land Use | C Factor | | | |
| Forest | 0.03 | | | |
| Shrub land | 0.03 | | | |
| Grassland | 0.01 | | | |
| Agricultural land | 0.21 | | | |
| Barren land | 0.45 | | | |
| Built-up | 0.01 | | | |
| Waterbody | 0.01 | | | |
| Snow glacier | 0.01 | | | |
| | | | | |

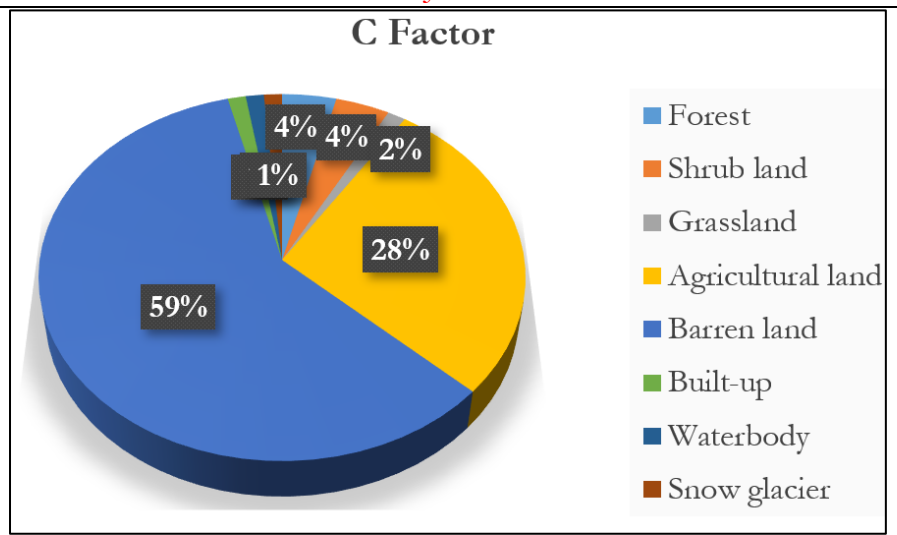


Figure 8: Land cover distribution in the study area

Support Factor:

The P-factor was calculated based on the corresponding land use and slope percentage. A support value of 1 was assigned to classes other than agriculture, regardless of slope and extent. The huge expanse of the agricultural land includes topography ranging from level 0 to 11% gently sloping. Contour farming, terracing, and strip cropping are some of the most well-known and well-researched management methods as shown in Table 5. The slope, expressed as percentage, was used to determine the agriculture extent in relation to the slope as shown in Figure 10.

Table 5: Values of P- Factor according to Soil Conservation Practice

| Slope% | Strip Cropping | Contour Cropping | Terrace Cropping | |
|-----------|----------------|------------------|------------------|--------------------|
| | | | Bench | Broad-based |
| 0-7.0 | 0.27 | 0.55 | 0.10 | 0.12 |
| 7.0-11.3 | 0.30 | 0.60 | 0.10 | 0.12 |
| 11.3-17.6 | 0.40 | 0.80 | 0.10 | 0.16 |
| 17.6-26.8 | 0.45 | 0.90 | 0.12 | 0.18 |
| >26.8 | 0.50 | 1.00 | 0.14 | 0.20 |



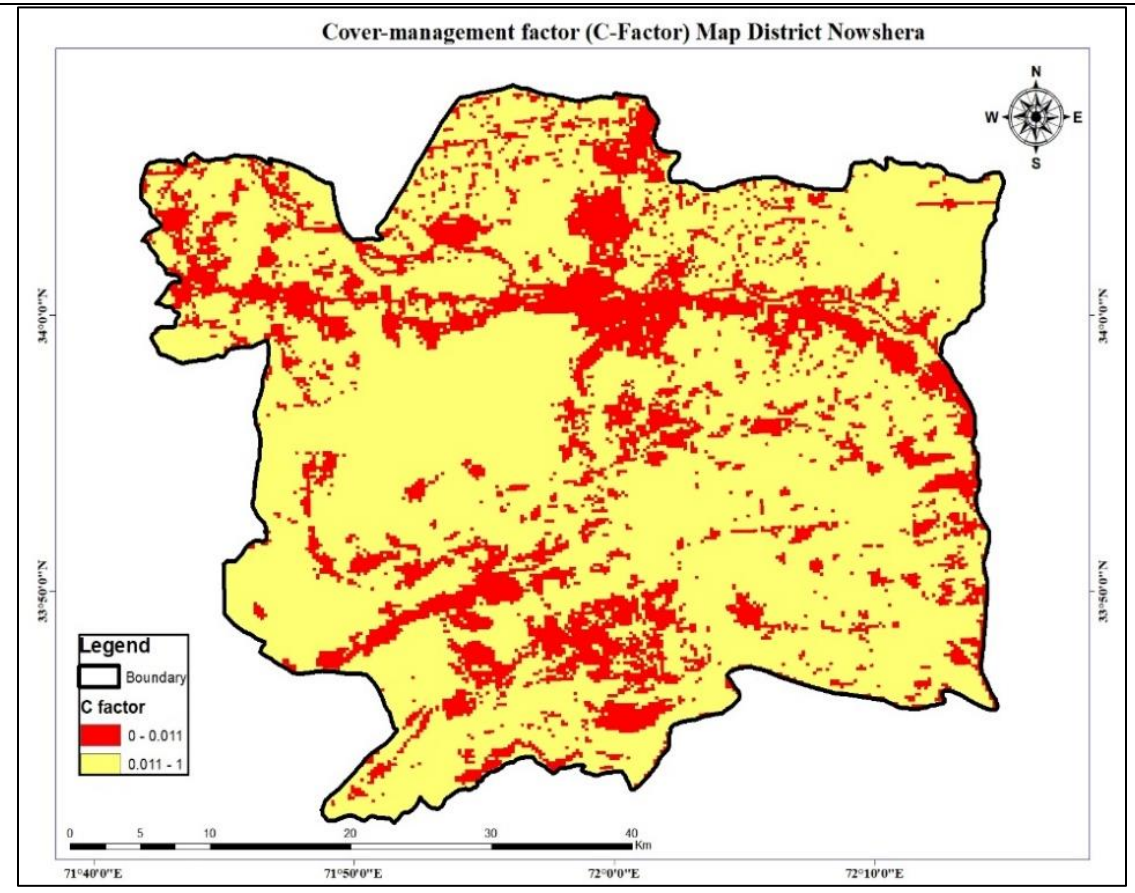


Figure 9: Crop factor (C) estimation in the study area

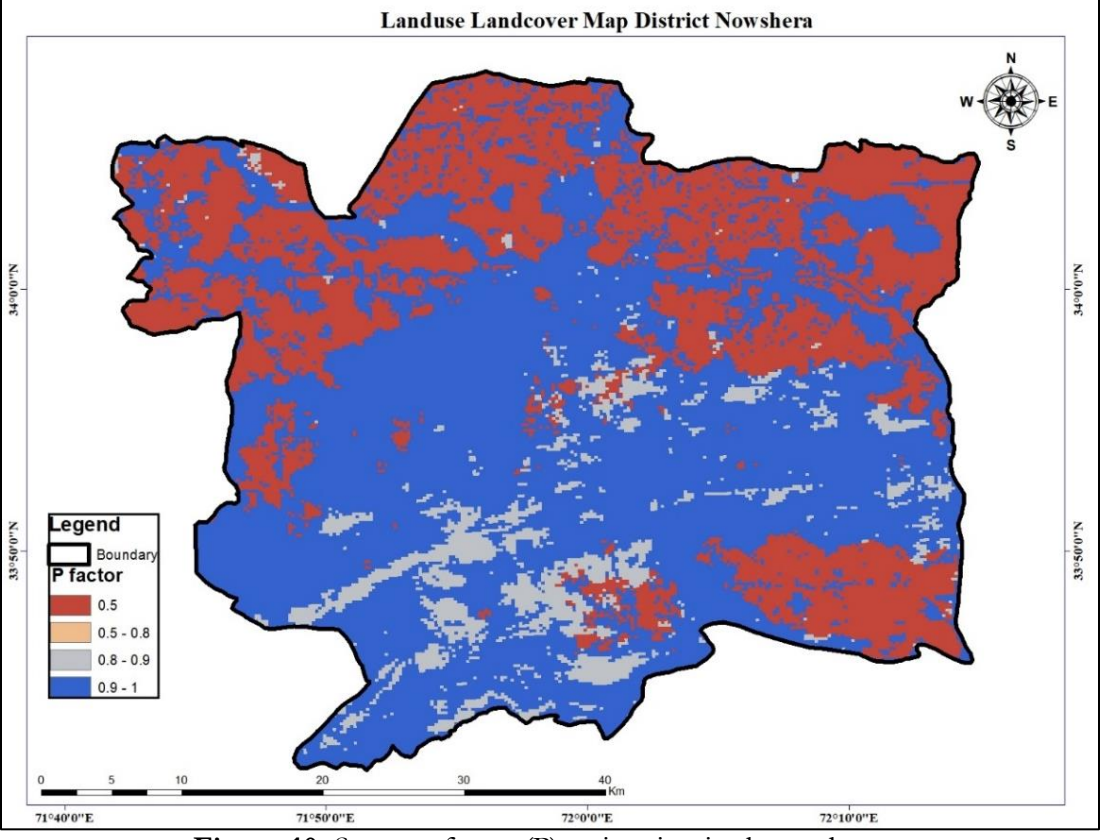


Figure 10: Support factor (P) estimation in the study area



Average Annual Soil Loss (A) Estimation:

The research region exhibits different degrees of soil erosion due to its diverse topography and undulating landscape. The average yearly soil loss varies from 0 to 263,618 tons/acre/year. In the Raster Calculator, all the layers were multiplied, resulting in erosion rates categorized into four classes: Low Erosion (0-0.5), Moderate Erosion (0.5-2.5), High Erosion (2.5-8.9), and Very Heavy Erosion (8.9-21.6), as depicted in Figure 11. According to the current study, the majority of hilly and arid regions are vulnerable to significant soil erosion. In the research area, a significant rate of soil erosion is also being caused by extensive deforestation.

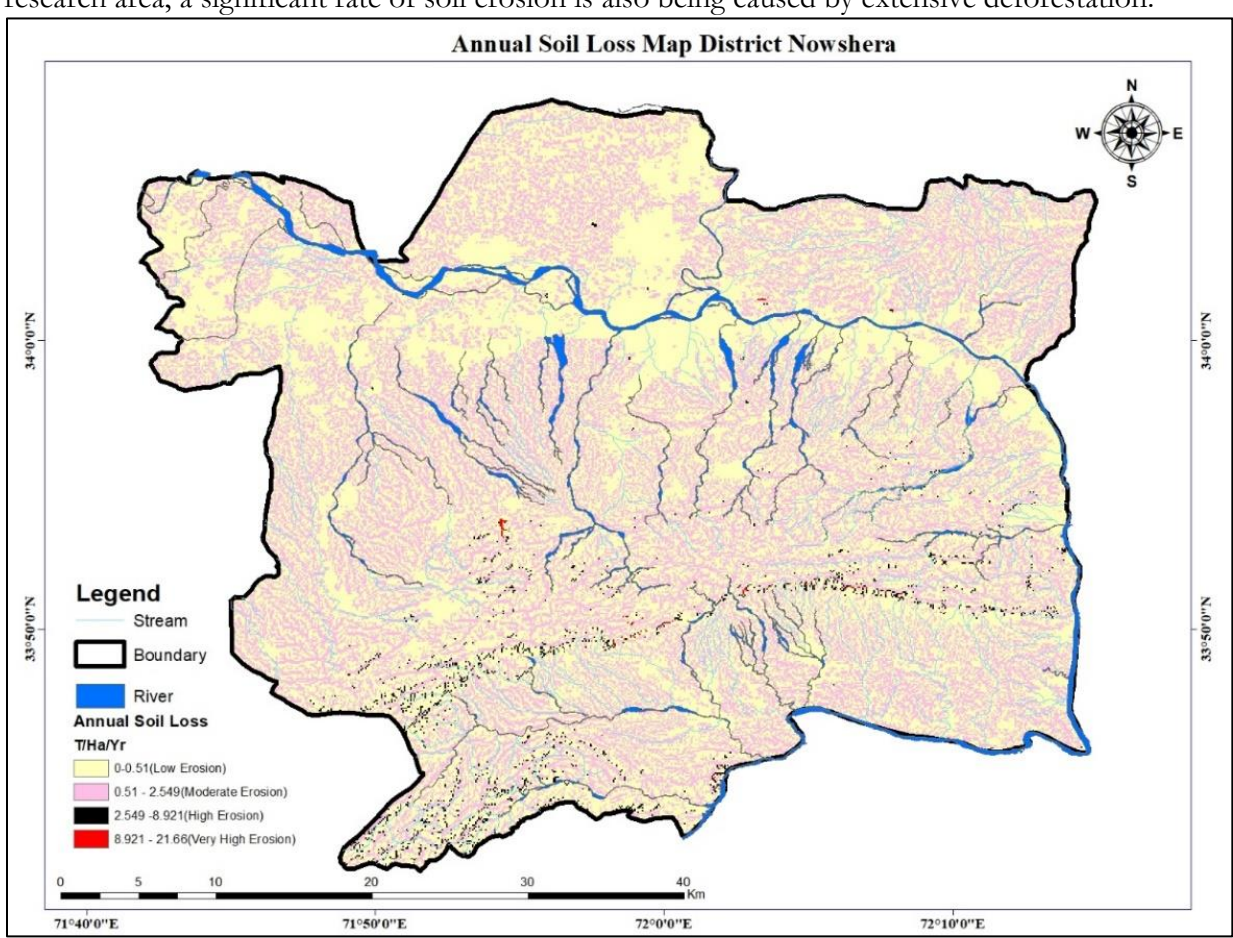


Figure 11: Average annual soil loss (A) in the study area.

Validation of the Results with Local and Global Studies:

The results of this study were compared with related investigations carried out in the adjacent regions, showing close alignment with previous studies at the watershed level. According to a study carried out at the Fateh Jang watershed, the rate of soil loss for uncultivated land was 17-41 tons/ha/year for slopes of roughly 1-10% in the area, whereas the rate was significantly lower (9-26 tons/ha/year) for vegetative land [25]. The rate of soil loss was found to be between 0.1 and 8 tons/ha/year in another study that used RUSLE to quantify soil loss for plain area soils in a small hilly watershed [26]. The watershed's average annual soil loss rate over its 13 hectares of total area was 19.1 tons per hectare. Steep slopes were responsible for around 74% of soil loss [17]. However, the result of current study, the Nowshera district of Pakistan is more vulnerable to soil erosion than the Potohar region.

High rates of erosion were predicted by [27] in the Kali River basin in Karnataka, India. The identifications of regions that are vulnerable to elevated soil erosion on steep terrains and mountain slopes highlight the significant influence of topographic features on affecting soil water erosion. In another study [28], reported significant soil erosion in the steep inclines of the



hilly area of the Indian Muthirapuzha River basin. Significant soil loss was estimated by [29] in Northwestern Ethiopia's steeply sloping terrain. While, the findings of this research are consistent with those of other studies carried out under comparable circumstances in other geographic locations.

Discussion:

Soil erosion is a geomorphic process that leads to removal of topsoil, consequently reducing the fertility [30]. An estimated 10 million hectares of arable land face errosion each year [31] making large areas of land unusable for cultivation globally [32]. The main causes of soil erosion, which heightened land degradation, include under-developed geology, human-induced intercession over the delicate slope, explosive population growth, unplanned alterations in land use land cover (LULC), and climatic conditions ranging from humid to sub-humid [33][34]. A widely accepted method for assessing soil erosion is using the Revised Universal Soil Loss Equation (RUSLE) model [16] due to its usefulness, accuracy, and legitimacy. Estimating soil loss is essential for managing agriculture and water, including the movement and storage of sediment [35]. Thus, this paper aims to estimate the dangers of soil erosion using the RUSLE model in the district Nowshera, Pakistan.

Many models are available to estimate soil erosion, however, the input data for each model varies greatly. RUSLE, however, is frequently used to calculate the risk of soil erosion [36]. Combining GIS and remote sensing with RUSLE enhances its reliability by providing a cell-by-cell (Raster) visual representation of risk zones [37]. The decision-making authorities can create plans and strategies for reducing soil erosion risk in certain zones with the use of the soil erosion risk map. GIS technology is used to spatially model and evaluate the RUSLE, which is a helpful tool for calculating soil erosion rates. This is a helpful tool for calculating soil erosion rates and may also be utilized to replicate erosion scenarios and pinpoint high-risk locations for erosion. It can access decision-making processes intended to reduce and manage soil erosion [38][39]. Over 76% of Pakistan's land is susceptible to erosion from wind and water[40]. Out of 23 million hectares, over 11 million hectares of suitable agricultural land are subject to erosion by water. Around 40 million tons of soil are eroded annually by the Indus River System in the upper catchment areas of the Hindu Kush, Himalayas, and Karakoram [41]. This causes siltation in the Mangla and Terbela dams, reducing the lifespan and capacity of the aforementioned multipurpose dams, impacting availability and electrical output [42].

The study utilized the Raster Calculator tool, a geospatial analysis tool within ArcGIS, to assess the degree of soil erosion. The study utilized the Raster Calculator tool, a geospatial analysis tool within ArcGIS, to assess the degree of soil erosion. The results were then divided into four classes according to the rate of erosion: low erosion (0-0.5), moderate erosion (0.5-2.5), high erosion (2.5-8.9), and very heavy erosion (8.9-21.6). Steep slopes were a defining feature of the areas experiencing the greatest erosion, especially along the water channels in the southern portion of the study area. The rates of soil loss in these locations increased from 0.5 to 2.5 tons per hectare per year during 2020. "Soil loss tolerance" describes the maximum amount of soil erosion that may be tolerated without adversely affecting the amount of food that can be produced. In tropical areas, the maximum rate of soil loss permitted is ten tons per hectare per year. Nerly 60% of the research area is below the soil tolerance limit based on these requirements.

The study results offer insightful information about which areas are most vulnerable to the risks associated with soil erosion. Consequently, this research helps with the creation of conservation plans at the regional level and has the potential to be expanded to the international level to create comprehensive plans for soil conservation. The elements that lead to soil erosion and the techniques employed to measure them must be carefully taken into account when assessing soil erosion. It also involves intricate models that are difficult to create and operate without a lot of computational power and knowledge. There is a chance that uncertainties in the



parameterization and input data will impact these models' accuracy. Therefore, for the proper evaluation of soil loss, sufficient and current information together with careful analysis of the elements for the determination of the RUSLE parameters are necessary.

Conclusions:

The areas exposed to high erosion risk can be precisely determined by using empirical soil erosion models, which, despite their relative simplicity, are easy to comprehend physically and require few resources. In this article, the potential zones for soil erosion in the district Nowshera, Pakistan are estimated by the use of empirical soil erosion model, such as RUSLE combined with GIS. By using the Weighted Index Overlay (WIO) approach, the land can be categorized into several zones according to the likelihood of soil erosion, which is eventually useful in determining the best course of action for protection. This study shows that GIS is a useful tool for estimating erosion loss and evaluating soil erosion. The following are the significant conclusions of the present study:

- The average yearly soil loss was estimated up to 263,618 tons/acre/year, with the highest soil erosion occurring in the vicinity of steep slopes and river systems. The research area is particularly vulnerable to erosion due to its uneven terrain and intricate drainage system.
- The construction of factories, housing buildings, and public amusement parks is one example of infrastructure development that has accelerated soil erosion. The continuous erosion of the soil may result in siltation in the canals and associated barrages, decreasing their water-carrying capacity and perhaps posing a risk of flooding in the area.
- Building terraces is necessary to stop erosion on high slopes, even though it could
 interfere with farming operations. Intelligent crop selection, considering the soil's
 potential, is crucial to prevent soil degradation. Intensive agriculture should be avoided
 as it can further degrade the soil quality.
- Zero tillage must take the place of the tillage technique. Adopting cropping strategies that maximize soil conservation is crucial. To preserve moisture throughout the summer season, mulching needs to be promoted. It is imperative to strategically arrange the cropping pattern to minimize the impact of wind. It is proposed that cross-slope farming support methods can lessen the amount of sediment that ends up on the surface. The findings of this research provide valuable insights for ecosystem protection and management, serving as a foundation for planning strategies worldwide.

Acknowledgment. Nil

Author's Contribution: Intisham Khan is the main and corresponding author of the Research, Muzamil Khan, Muhammad Fahad Bilal, Shahid Ghazi, and Kashif Khan contribute to the reviewing and editing of the writeup.

Conflict of Interest: The authors declare they have no conflict of interest in publishing this manuscript in this Journal.

References:

- [1] Q. Ulain, S. M. Ali, A. A. Shah, K. M. J. Iqbal, W. Ullah, and M. A. U. R. Tariq, "Identification of Soil Erosion-Based Degraded Land Areas by Employing a Geographic Information System—A Case Study of Pakistan for 1990–2020," Sustain. 2022, Vol. 14, Page 11888, vol. 14, no. 19, p. 11888, Sep. 2022, doi: 10.3390/SU141911888.
- [2] D. Mandal, M. Chandrakala, N. M. Alam, T. Roy, and U. Mandal, "Assessment of soil quality and productivity in different phases of soil erosion with the focus on land degradation neutrality in tropical humid region of India," CATENA, vol. 204, p. 105440, Sep. 2021, doi: 10.1016/J.CATENA.2021.105440.
- [3] S. Siddiqui, M. W. A. Safi, A. Tariq, N. U. Rehman, and S. W. Haider, "GIS Based Universal Soil Erosion Estimation in District Chakwal Punjab, Pakistan," Int. J. Econ.

- Environ. Geol., vol. 11, no. 2, pp. 30–36, Sep. 2020, doi: 10.46660/IJEEG.VOL11.ISS2.2020.443.
- [4] J. Poesen, "Soil erosion in the Anthropocene: Research needs," Earth Surf. Process. Landforms, vol. 43, no. 1, pp. 64–84, Jan. 2018, doi: 10.1002/ESP.4250.
- [5] K. T. Osman, "Soil Erosion by Water," Soil Degrad. Conserv. Remediat., pp. 69–101, 2014, doi: 10.1007/978-94-007-7590-9_3.
- [6] P. A. Ochoa, A. Fries, D. Mejía, J. I. Burneo, J. D. Ruíz-Sinoga, and A. Cerdà, "Effects of climate, land cover and topography on soil erosion risk in a semiarid basin of the Andes," CATENA, vol. 140, pp. 31–42, May 2016, doi: 10.1016/J.CATENA.2016.01.011.
- [7] N. A. S. Bashir, A. Javed, I. Bibi, "Soil and water conservation," Pakistan," Univ. Agric. Faisalabad, pp. 263–286, 2017.
- [8] J. Zhou et al., "The long-term uncertainty of biodegradable mulch film residues and associated microplastics pollution on plant-soil health," J. Hazard. Mater., vol. 442, p. 130055, Jan. 2023, doi: 10.1016/J.JHAZMAT.2022.130055.
- [9] B. Yadav et al., "Modeling and Assessment of Land Degradation Vulnerability in Arid Ecosystem of Rajasthan Using Analytical Hierarchy Process and Geospatial Techniques," L. 2023, Vol. 12, Page 106, vol. 12, no. 1, p. 106, Dec. 2022, doi: 10.3390/LAND12010106.
- [10] M. R. Rahman, Z. H. Shi, and C. Chongfa, "Soil erosion hazard evaluation—An integrated use of remote sensing, GIS and statistical approaches with biophysical parameters towards management strategies," Ecol. Modell., vol. 220, no. 13–14, pp. 1724–1734, Jul. 2009, doi: 10.1016/J.ECOLMODEL.2009.04.004.
- [11] A. R. Vaezi, M. Ahmadi, and A. Cerdà, "Contribution of raindrop impact to the change of soil physical properties and water erosion under semi-arid rainfalls," Sci. Total Environ., vol. 583, pp. 382–392, Apr. 2017, doi: 10.1016/J.SCITOTENV.2017.01.078.
- [12] F. Sajedi-Hosseini, B. Choubin, K. Solaimani, A. Cerdà, and A. Kavian, "Spatial prediction of soil erosion susceptibility using a fuzzy analytical network process: Application of the fuzzy decision making trial and evaluation laboratory approach," L. Degrad. Dev., vol. 29, no. 9, pp. 3092–3103, Sep. 2018, doi: 10.1002/LDR.3058.
- [13] D. D. Alexakis, E. Tapoglou, A. E. K. Vozinaki, and I. K. Tsanis, "Integrated Use of Satellite Remote Sensing, Artificial Neural Networks, Field Spectroscopy, and GIS in Estimating Crucial Soil Parameters in Terms of Soil Erosion," Remote Sens. 2019, Vol. 11, Page 1106, vol. 11, no. 9, p. 1106, May 2019, doi: 10.3390/RS11091106.
- [14] I. Gitas, K. Douros, C. Minakou, G. N. Silleos, and C. Karydas, "Multi-temporal soil erosion risk assessment in N. Chalkidiki using a modified USLE raster model.," 2009.
- [15] S. Kumar et al., "Estimation of soil erosion in indo-gangetic region using revised universal soil loss equation (RUSLE) model and geospatial technology," Model. Earth Syst. Environ., vol. 9, no. 1, pp. 1251–1273, Mar. 2023, doi: 10.1007/S40808-022-01553-W/METRICS.
- [16] "Predicting rainfall erosion losses: a guide to conservation planning." Accessed: May 21, 2024. [Online]. Available: https://www3.epa.gov/npdes/pubs/ruslech2.pdf
- [17] S. Ullah, A. Ali, M. Iqbal, M. Javid, and M. Imran, "Geospatial assessment of soil erosion intensity and sediment yield: a case study of Potohar Region, Pakistan," Environ. Earth Sci., vol. 77, no. 19, pp. 1–13, Oct. 2018, doi: 10.1007/S12665-018-7867-7/METRICS.
- [18] M. Wynants, H. Solomon, P. Ndakidemi, and W. H. Blake, "Pinpointing areas of increased soil erosion risk following land cover change in the Lake Manyara catchment, Tanzania," Int. J. Appl. Earth Obs. Geoinf., vol. 71, pp. 1–8, Sep. 2018, doi: 10.1016/J.JAG.2018.05.008.
- [19] E. Z. Nyakatawa, K. C. Reddy, and J. L. Lemunyon, "Predicting soil erosion in



- conservation tillage cotton production systems using the revised universal soil loss equation (RUSLE)," Soil Tillage Res., vol. 57, no. 4, pp. 213–224, Jan. 2001, doi: 10.1016/S0167-1987(00)00178-1.
- [20] E. Burnett, B. A. Stewart, and A. L. Black, "Regional Effects of Soil Erosion on Crop Productivity—Great Plains," Soil Eros. Crop Product., pp. 285–304, Jan. 2015, doi: 10.2134/1985.SOILEROSIONANDCROP.C17.
- [21] E. H. Erdogan, G. Erpul, and I. Bayramin, "Use of USLE/GIS methodology for predicting soil loss in a semiarid agricultural watershed," Environ. Monit. Assess., vol. 131, no. 1–3, pp. 153–161, Aug. 2007, doi: 10.1007/S10661-006-9464-6/METRICS.
- [22] M. Hrabalíková and M. Janeček, "Comparison of different approaches to LS factor calculations based on a measured soil loss under simulated rainfall.," https://swr.agriculturejournals.cz/doi/10.17221/222/2015-SWR.html, vol. 12, no. 2, pp. 69–77, 2017, doi: 10.17221/222/2015-SWR.
- [23] F. Mushtaq and M. G. N. Lala, "Assessment of hydrological response as a function of LULC change and climatic variability in the catchment of the Wular Lake, J&K, using geospatial technique," Environ. Earth Sci., vol. 76, no. 22, pp. 1–19, Nov. 2017, doi: 10.1007/S12665-017-7065-Z/METRICS.
- [24] J. M. van der Knijff, J. Younis, and A. P. J. de Roo, "LISFLOOD: a GIS-based distributed model for river basin scale water balance and flood simulation," Int. J. Geogr. Inf. Sci., vol. 24, no. 2, pp. 189–212, Feb. 2010, doi: 10.1080/13658810802549154.
- [25] A. Ashraf, "Risk modeling of soil erosion under different land use and rainfall conditions in Soan river basin, sub-Himalayan region and mitigation options," Model. Earth Syst. Environ., vol. 6, no. 1, pp. 417–428, Mar. 2020, doi: 10.1007/S40808-019-00689-6/METRICS.
- [26] A. Maqsoom et al., "Geospatial Assessment of Soil Erosion Intensity and Sediment Yield Using the Revised Universal Soil Loss Equation (RUSLE) Model," ISPRS Int. J. Geo-Information 2020, Vol. 9, Page 356, vol. 9, no. 6, p. 356, May 2020, doi: 10.3390/IJGI9060356.
- [27] V. J. Markose and K. S. Jayappa, "Soil loss estimation and prioritization of subwatersheds of Kali River basin, Karnataka, India, using RUSLE and GIS," Environ. Monit. Assess., vol. 188, no. 4, pp. 1–16, Apr. 2016, doi: 10.1007/S10661-016-5218-2/METRICS.
- [28] J. Thomas, S. Joseph, and K. P. Thrivikramji, "Assessment of soil erosion in a tropical mountain river basin of the southern Western Ghats, India using RUSLE and GIS," Geosci. Front., vol. 9, no. 3, pp. 893–906, May 2018, doi: 10.1016/J.GSF.2017.05.011.
- [29] M. Zerihun, M. S. Mohammedyasin, D. Sewnet, A. A. Adem, and M. Lakew, "Assessment of soil erosion using RUSLE, GIS and remote sensing in NW Ethiopia," Geoderma Reg., vol. 12, pp. 83–90, Mar. 2018, doi: 10.1016/J.GEODRS.2018.01.002.
- [30] P. Ochoa-Cueva, A. Fries, P. Montesinos, J. A. Rodríguez-Díaz, and J. Boll, "Spatial Estimation of Soil Erosion Risk by Land-cover Change in the Andes OF Southern Ecuador," L. Degrad. Dev., vol. 26, no. 6, pp. 565–573, Aug. 2015, doi: 10.1002/LDR.2219.
- [31] M. Wagari and H. Tamiru, "RUSLE Model Based Annual Soil Loss Quantification for Soil Erosion Protection: A Case of Fincha Catchment, Ethiopia," Air, Soil Water Res., vol. 14, Oct. 2021, doi: 10.1177/11786221211046234/ASSET/IMAGES/LARGE/10.1177_11786221211046 234-FIG10.JPEG.
- [32] V. Prasannakumar, H. Vijith, S. Abinod, and N. Geetha, "Estimation of soil erosion risk within a small mountainous sub-watershed in Kerala, India, using Revised Universal Soil Loss Equation (RUSLE) and geo-information technology," Geosci. Front., vol. 3, no. 2,



- pp. 209–215, Mar. 2012, doi: 10.1016/J.GSF.2011.11.003.
- [33] T. S. Abdulkadir et al., "Quantitative analysis of soil erosion causative factors for susceptibility assessment in a complex watershed," Cogent Eng., vol. 6, no. 1, Jan. 2019, doi: 10.1080/23311916.2019.1594506.
- [34] R. Chakrabortty, B. Pradhan, P. Mondal, and S. C. Pal, "The use of RUSLE and GCMs to predict potential soil erosion associated with climate change in a monsoon-dominated region of eastern India," Arab. J. Geosci., vol. 13, no. 20, pp. 1–20, Oct. 2020, doi: 10.1007/S12517-020-06033-Y/METRICS.
- [35] "Modeling soil erosion processes in watersheds and the relation between soil loss with geomorphic and chemical parameters Fingerprint King Fahd University of Petroleum & Minerals." Accessed: May 21, 2024. [Online]. Available: https://pure.kfupm.edu.sa/en/publications/modeling-soil-erosion-processes-in-watersheds-and-the-relation-be-2/fingerprints/
- [36] T. G. Pham, J. Degener, and M. Kappas, "Integrated universal soil loss equation (USLE) and Geographical Information System (GIS) for soil erosion estimation in A Sap basin: Central Vietnam," Int. Soil Water Conserv. Res., vol. 6, no. 2, pp. 99–110, Jun. 2018, doi: 10.1016/J.ISWCR.2018.01.001.
- [37] P. Thapa, "Spatial Estimation of Soil Erosion Using RUSLE Modeling: A case study of Dolakha District, Nepal," Jul. 2020, doi: 10.21203/RS.3.RS-25478/V4.
- [38] S. C. Pal and R. Chakrabortty, "Modeling of water induced surface soil erosion and the potential risk zone prediction in a sub-tropical watershed of Eastern India," Model. Earth Syst. Environ., vol. 5, no. 2, pp. 369–393, Jun. 2019, doi: 10.1007/S40808-018-0540-Z/METRICS.
- [39] G. Thakuriah, "Correction to: GIS-based revised universal soil loss equation for estimating annual soil erosion: a case of lower Kulsi basin, India (SN Applied Sciences, (2023), 5, 3, (81), 10.1007/s42452-023-05303-0)," SN Appl. Sci., vol. 5, no. 4, pp. 1–1, Apr. 2023, doi: 10.1007/S42452-023-05317-8/METRICS.
- [40] M. B. Baig, S. A. Shahid, and G. S. Straquadine, "Making rainfed agriculture sustainable through environmental friendly technologies in Pakistan: A review," Int. Soil Water Conserv. Res., vol. 1, no. 2, pp. 36–52, Sep. 2013, doi: 10.1016/S2095-6339(15)30038-1.
- [41] A. Khan, A. U. Rahman, and S. Mahmood, "Spatial estimation of soil erosion risk using RUSLE model in District Swat, Eastern Hindu Kush, Pakistan," J. Water Clim. Chang., vol. 14, no. 6, pp. 1881–1899, Jun. 2023, doi: 10.2166/WCC.2023.495/1246359/JWC0141881.PDF.
- [42] M. Irshad, J. Ali, Faridullah, and A. Egrinya Eneji, "Chemical properties of soil and runoff water under different land uses in Abbottabad, Pakistan," Environ. Earth Sci., vol. 74, no. 4, pp. 3501–3506, Aug. 2015, doi: 10.1007/S12665-015-4386-7/METRICS.



Copyright © by authors and 50Sea. This work is licensed under Creative Commons Attribution 4.0 International License.